


In presenting the dissertation as a partial fulfillment of the requirements for an advanced degree from the Georgia Institute of Technology, I agree that the Library of the Institute shall make it available for inspection and circulation in accordance with its regulations governing materials of this type. I agree that permission to copy from, or to publish from, this dissertation may be granted by the professor under whose direction it was written, or, in his absence, by the Dean of the Graduate Division when such copying or publication is solely for scholarly purposes and does not involve potential financial gain. It is understood that any copying from, or publication of, this dissertation which involves potential financial gain will not be allowed without written permission.



3/17/65

b

A STUDY OF IRON IN CLAY MINERALS USING MÖSSBAUER SPECTROSCOPY

A THESIS

Presented to

The Faculty of the Graduate Division

by

Thomas Edward Pecuil

In Partial Fulfillment

of the Requirements for the Degree

Master of Science in Ceramic Engineering

Georgia Institute of Technology

July, 1966

A STUDY OF IRON IN CLAY MINERALS USING MÖSSBAUER SPECTROSCOPY

Approved.

Chairman

Date approved by Chairman: Aug 30, 1966

ACKNOWLEDGMENTS

I am very fortunate to have had the understanding, guidance, and encouragement of Dr. C. E. Weaver throughout the critical times of my graduate work. A special thanks to Dr. J. M. Wampler, without whose assistance the first experiment would never have been performed. My appreciation is also expressed to Dr. Lane Mitchell and Mr. Thomas Mackrovitch, both of whom always found time to help and guide me. And finally, my sincere thanks to Miss Ginga Jacobson for her excellent typing.

TABLE OF CONTENTS

	Page
ACKNOWLEDGMENTS	ii
LIST OF TABLES	iv
LIST OF FIGURES	v
SUMMARY	vi
CHAPTER	
I. INTRODUCTION	1
Historical and Literature Review	2
II. INSTRUMENTATION	7
Procedure	11
III. DISCUSSION OF RESULTS	12
Clay Samples	15
2:1 Dioctahedral (Figure 7)	15
2:1 Chain (Figure 8)	17
1:1 Trioctahedral (Figure 9)	20
2:1 Trioctahedral Minerals (Figures 10 and 11)	22
Iron Minerals (Figure 12)	25
IV. CONCLUSIONS AND RECOMMENDATIONS	31
The Following Improvements in Research	
Techniques are Recommended	31
A. Samples	31
B. Equipment	32
C. Research	32
BIBLIOGRAPHY	33

LIST OF TABLES

Table		Page
1.	Mössbauer Parameters Determined in This Work for Clays and Associated Minerals	13

LIST OF FIGURES

Figure		Page
1.	Energy Level Diagram and Typical Spectrum for Isomer Shift	4
2.	Energy Level Diagram and Typical Spectrum for Quadrupole Splitting	4
3.	Energy Level Diagram and Typical Spectrum for Magnetic Splitting	4
4.	Photograph of Mössbauer Transducer	8
5.	Decay Scheme for Co ⁵⁷	9
6.	Mössbauer Effect Spectrometer	10
7.	Mössbauer Spectra of 2:1 Dioctahedral Clays Vertical Scale in Counts/Minute	16
8.	Mössbauer Spectra of Chain Structure Clays Vertical Scale in Counts/Minute	19
9.	Mössbauer Spectra of 1:1 Trioctahedral Clays Vertical Scale in Counts/Minute	21
10.	Mössbauer Spectra of Biotite Vertical Scale in Counts/Minute	24
11.	Mössbauer Spectra of Ferrianite and Griffithite Vertical Scale in Counts/Minute	24
12.	Mössbauer Spectra of Siderite, Fe-Kaolin and Goethite Vertical Scale in Counts/Minute	26
13.	Schematic Diagram of the Gamma-ray Source Showing the Effect of Source Location on Line Broadening	30

SUMMARY

The Mössbauer effect, recoilless nuclear resonance absorption of gamma radiation by nuclei of atoms bound in solids, has made it possible to observe characteristic absorption spectra which are highly sensitive to small variations in the nuclear environment. A recoil-free condition exists when the absorption (or emission) of a gamma ray occurs without transferring energy to change the state of excitation of the lattice. The recoil momentum is taken up by the lattice and the recoil energy associated with the translational motion of the lattice is negligible compared to the natural line width of the gamma ray. The exceptional energy resolution of these recoil-free transitions allows the detection of very small line shifts and splittings caused by the interaction of the nuclei with electric and magnetic fields created by the atomic electrons.

Studies of the resonant absorption of gamma rays by Fe^{57} nuclei in various compounds and minerals has indicated that the magnitude of the isomer shift and electric quadrupole splitting are functions of the valence state of the iron. The isomer shift depends on the charge density of the electrons at the nucleus. The quadrupole splitting arises from asymmetry of the electric field gradient at a nuclear site and thus tells something of the neighboring ions in a lattice.

Mössbauer absorption spectra of iron were obtained from clay minerals with 2:1 sheet, 1:1 sheet, and chain structures. All three basic structural types have dioctahedral (two of the three octahedral positions filled) and trioctahedral (all three octahedral positions filled) members.

The effects of iron oxides and hydroxides external to the lattice were also determined.

It was possible to identify the oxidation states of iron (Fe^{+2} and Fe^{+3}), singularly or when both are present, from their characteristic isomer shifts and quadrupole splittings. Values of the isomer shifts and quadrupole splittings were greater for trioctahedral clays, indicating greater asymmetry than the dioctahedral clays. Results from a synthetic biotite sample (containing tetrahedral iron) indicated that tetrahedral and octahedral coordination could be resolved for an iron ion. Studies of iron oxyhydroxides helped to show that an iron-kaolin was a mixture of fine particle α $\text{FeO}(\text{OH})$ and kaolin, and not a kaolin with iron in the lattice.

CHAPTER I

INTRODUCTION

Most of the clay minerals contain iron in their lattice and usually contain an admixture or coating of iron oxides. It is difficult and often impossible to determine if the iron associated with clays is in the lattice or external. Even if this can be established, there is no means of knowing where the iron occurs in the lattice (tetrahedral or octahedral coordination). It is also usual for most clays to have iron present in both the Fe^{+2} and Fe^{+3} state. In addition, the clay minerals have three different structural arrangements--2:1 sheet, 1:1 sheet, and chain. All three basic structural types have dioctahedral (two of the three octahedral positions filled) and trioctahedral (all three octahedral positions filled) members.

In nature, clay minerals are commonly found in mixtures of varying proportions. Usually these mixtures cannot be separated, and though mineral identification and percentages can be found, there is no direct method of determining anything about the chemical composition of the specific clay minerals in the mixture. It would be of considerable value to be able to determine the content and valence state of the iron in specific clays, particularly when in mixtures.

The purpose of this work is to obtain Mössbauer spectra of clays representative of the three structural types, including samples where iron is in either tetrahedral or octahedral coordination or in both.

Historical and Literature Review

The discovery of a new phenomenon, the recoilless nuclear resonance absorption of gamma radiation, now called the "Mössbauer Effect," was published in 1958 (Mössbauer, 1958). About a year later, research teams at the Argonne and Los Alamos National Laboratories, began to repeat and extend the originally reported work. These early experiments were performed with Ir^{191} . The discovery of the Mössbauer effect in Fe^{57} opened the field of recoil-free experiments to many laboratories and to greater exploration.

At the time of the Second International Conference on the Mössbauer Effect, September, 1961, approximately one hundred and fifty active contributors attended an informal meeting on the Mössbauer effect. A broader use of the new technique and applications to solid state physics was among the major topics discussed. A third conference, held in 1963 at Cornell University, illustrates the expanding range of the discovery. The discussions and topics had broadened to include relativity, magnetism, metallurgy, and chemistry.

Frauenfelder, who coordinated and arranged the scientific program for the second conference, provides a bibliography of work in this field in The Mössbauer Effect (1962). Wertheim (1963) has also compiled a list of references containing background, reviews, and applications of the Mössbauer effect.

Application of the Mössbauer effect to certain nuclei has made it possible to observe characteristic absorption spectra. A recoil-free condition exists when the absorption (or emission) of a gamma ray occurs without transferring energy to change the state of excitation of the lattice, i.e., a process whereby the whole energy of the nuclear transition goes

into (or comes from) the gamma ray. The recoil momentum is taken up by the lattice, and the recoil energy associated with the translational motion of the lattice is negligible compared to the natural line width of the gamma ray. "... when the lattice is not excited the widths of the nuclear levels involved in the transitions alone determine the line width of the zero-phonon component." (Wertheim, 1964).

In an experiment, the energy of the emitted radiation from a source moving toward an absorber is changed by $\frac{E v}{c}$ (Doppler shifted) where v is the component of velocity along the source-to-absorber direction. To obtain an absorption spectrum, the transmission of gamma rays through the absorber must be measured as a function of the Doppler velocity.

Very small line shifts and splittings caused by the interaction of the nuclei with electric and magnetic fields created by the atomic electrons are observable in the absorption spectra. There are three useful components of this interaction: the isomer shift, the nuclear electric quadrupole splitting, and the nuclear magnetic dipole splitting. The isomer shift is an interaction due to the charge density of the (negative) electrons at the (positive) nucleus (Kistner and Sunyar, 1960) (Figure 1). The quadrupole splitting depends on the asymmetry of the electric field gradient at the nuclear site (Figure 2). It has been reported (DeBenedetti, et al., 1961) that the splitting for Fe^{+3} is caused by the neighboring ions; however, for Fe^{+2} the relevant field gradient is related primarily to the electron distribution in the iron ion. A magnetic (Zeeman) splitting (Figure 3) results from interaction of the nuclear magnetic dipole moment with the magnetic field produced at the nuclear site by the atomic electrons (Hanna, et al., 1960). All of these properties enable one to deter-

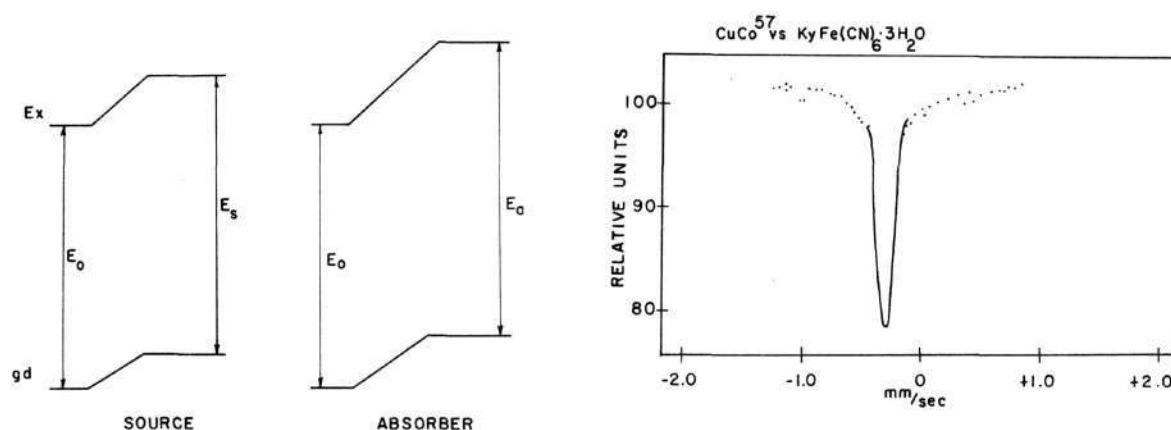


Figure 1. Energy Level Diagram and Typical Spectrum for Isomer Shift.

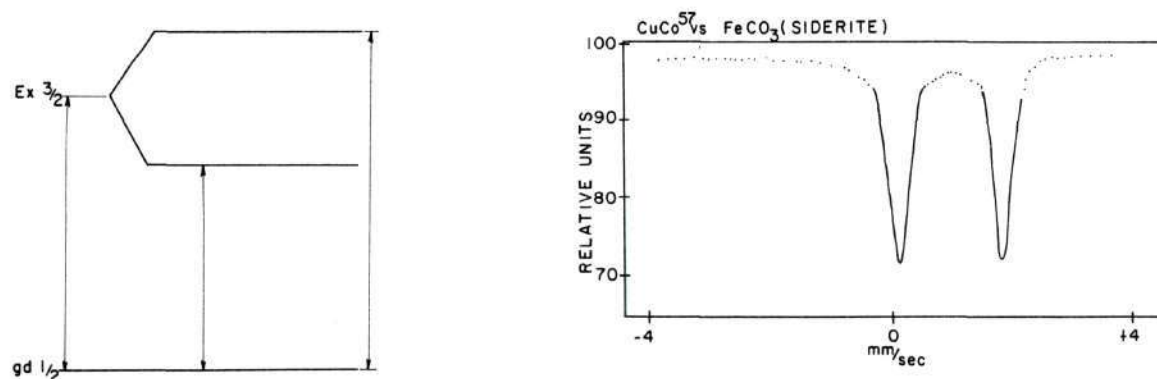


Figure 2. Energy Level Diagram and Typical Spectrum for Quadrupole Splitting.

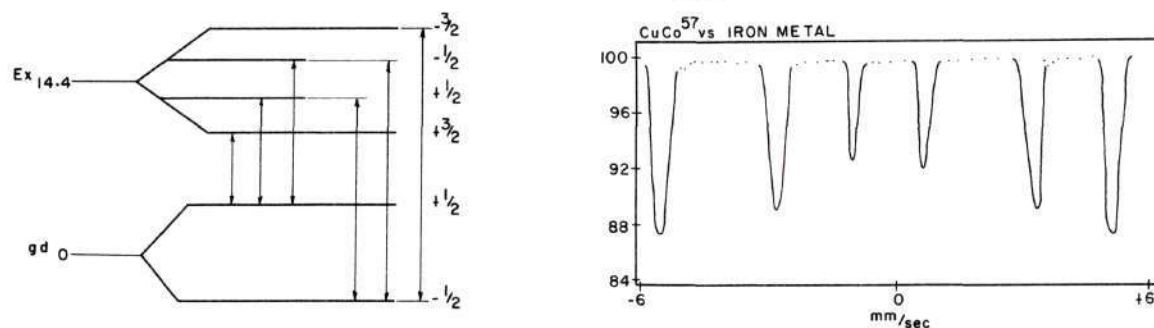


Figure 3. Energy Level Diagram and Typical Spectrum for Magnetic Splitting.

mine not only the presence of an element causing a characteristic spectrum, but also its oxidation state.

The isomer shift which is related to chemical bonding and changes in valence, and the quadrupole splitting which is sensitive to structural environment, are the prime considerations in this work.

The discovery of Mössbauer absorption by Fe^{57} opened the field to much greater study and produced numerous studies of Fe^{57} in various forms. Fe^{57} has a very narrow natural line width and is not greatly influenced by temperature changes, allowing room temperature experiments.

The quadrupole coupling and isomer shift have been determined for Fe^{57} bound in Fe_2O_3 (Kistner and Sunyar, 1960). A recent study of stone meteorites produced characteristic absorption patterns for the metallic phase, non-silicate iron-minerals, and iron-silicate minerals (Sprenkel-Segel and Hanna, 1964). Earlier work involving silicate minerals was done by Pollak, et al., (1962) with biotite, and expanded at a later time to other silicate minerals (DeCoster, et al., 1963). Herzenberg and Toms' (1966) study of various iron oxides and oxyhydroxides, is particularly pertinent to this work as most clays contain an admixture or coating of iron oxides. The list of iron compounds with their isomer shifts and quadrupole splittings has grown steadily (DeBenedetti, et al., 1961; Walker, et al., 1961; and Fluck, et al., 1963). From these data it can be shown that the characteristic isomer shift and quadrupole splitting can be associated with the valence state of the ion. The approximate range of values for room temperature experiments is as follows: the isomer shift (measured from the center of the iron metal pattern) for Fe^{+3} from + 0.0 through + 0.5 mm/second, for Fe^{+2} from + 1.0 through + 1.4 mm/second. Quadrupole

splittings for Fe^{+3} range from 0 through 0.5 mm/second and for Fe^{+2} from 0.40 through 1.7 mm/second. An exception occurs when an ion is in local cubic symmetry, for then no quadrupole splitting is observed. The values listed above will be helpful in making determinations of the valence state of the iron ion.

CHAPTER II

INSTRUMENTATION

A surplus Mössbauer transducer was obtained from Oak Ridge National Laboratory, Oak Ridge, Tennessee. The transducer provides the means of imparting a constant velocity to the sample. A 10 rpm synchronous motor operating a set of gears (maximum ratio 16:1) rotates a drive wheel which moves a constant velocity cam (Figure 4). Descriptions and illustrations of various constant velocity mechanisms are readily available (Frauenfelder, 1962). The constant velocity cam drives a lever arm attached to the sample holder and can move it through a distance of 5 mm. The cam is divided into four equal portions. One portion imparts a positive velocity to the sample ("positive velocity" means that the sample is moving toward the source); one portion imparts a negative velocity; and the two remaining intermediate portions are stationary (zero velocity) positions. A second synchronous motor (1 rpm) can be interchanged easily with the 10 rpm motor, permitting study of velocities from zero to 6 mm/second.

A suitable gamma ray source of Co^{57} , (10 mc) plated and annealed in copper was purchased from Nuclear Science and Engineering Corporation, Pittsburgh, Pennsylvania. Co^{57} , in the process of radioactive decay, generates a 14.4 Kev isomeric state of the decay product, Fe^{57} , capable of eliciting nuclear resonance absorption, "Mössbauer effect," in another nucleus of its own kind (Figure 5).

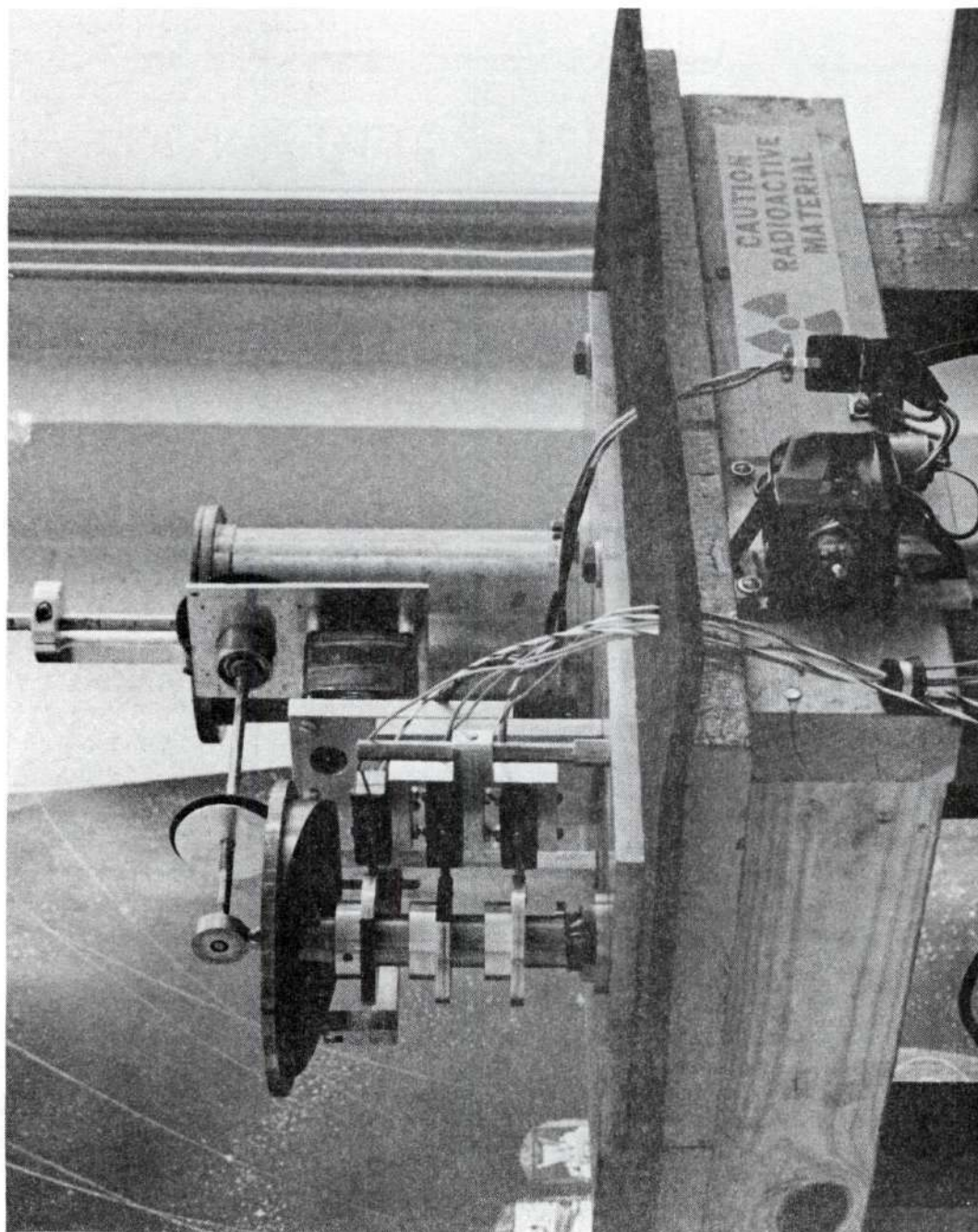


Figure 4. Photograph of Mössbauer Transducer.

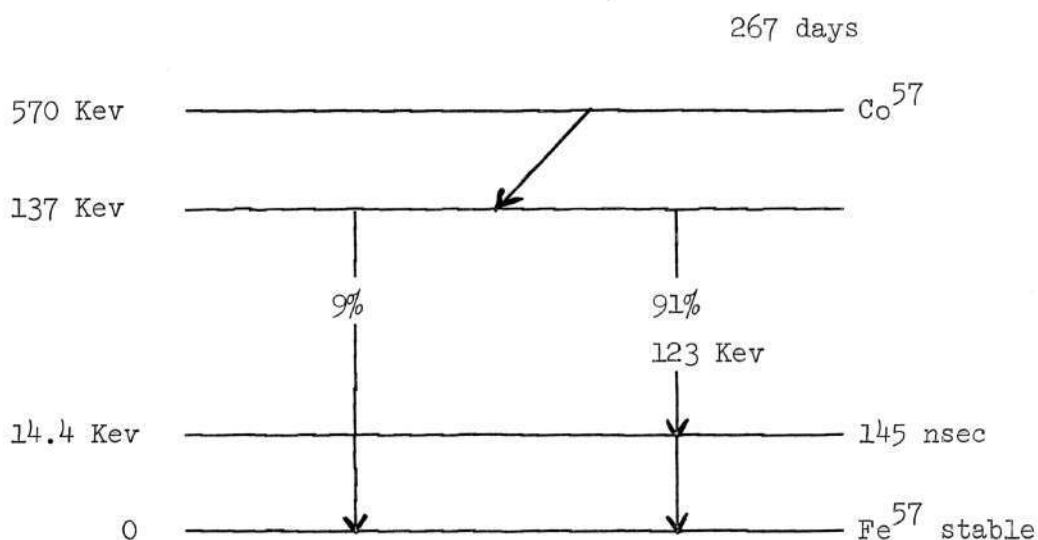


Figure 5. Decay Scheme for Co^{57}

To count the Mössbauer gamma rays, a double window gas flow proportional counter using 90 percent argon, 10 percent methane gas was built. The counter was made of 2 inch diameter aluminum tubing with a center wire of 0.003 inch diameter stainless steel, and .00025 inch aluminized mylar to cover the windows.

The signal from the proportional counter is amplified and sent to a single channel pulse height analyzer to discriminate against the K x-rays of iron and higher energy gamma radiation from the source. The selected signal from the pulse height analyzer is then sent to three scalers: one scaler collects counts for the positive velocity, one collects counts for the negative velocity, and the third scaler collects the stationary counts (Figure 6). Each scaler is controlled with microswitches operated by cams synchronized with the constant velocity cam (Figure 4).

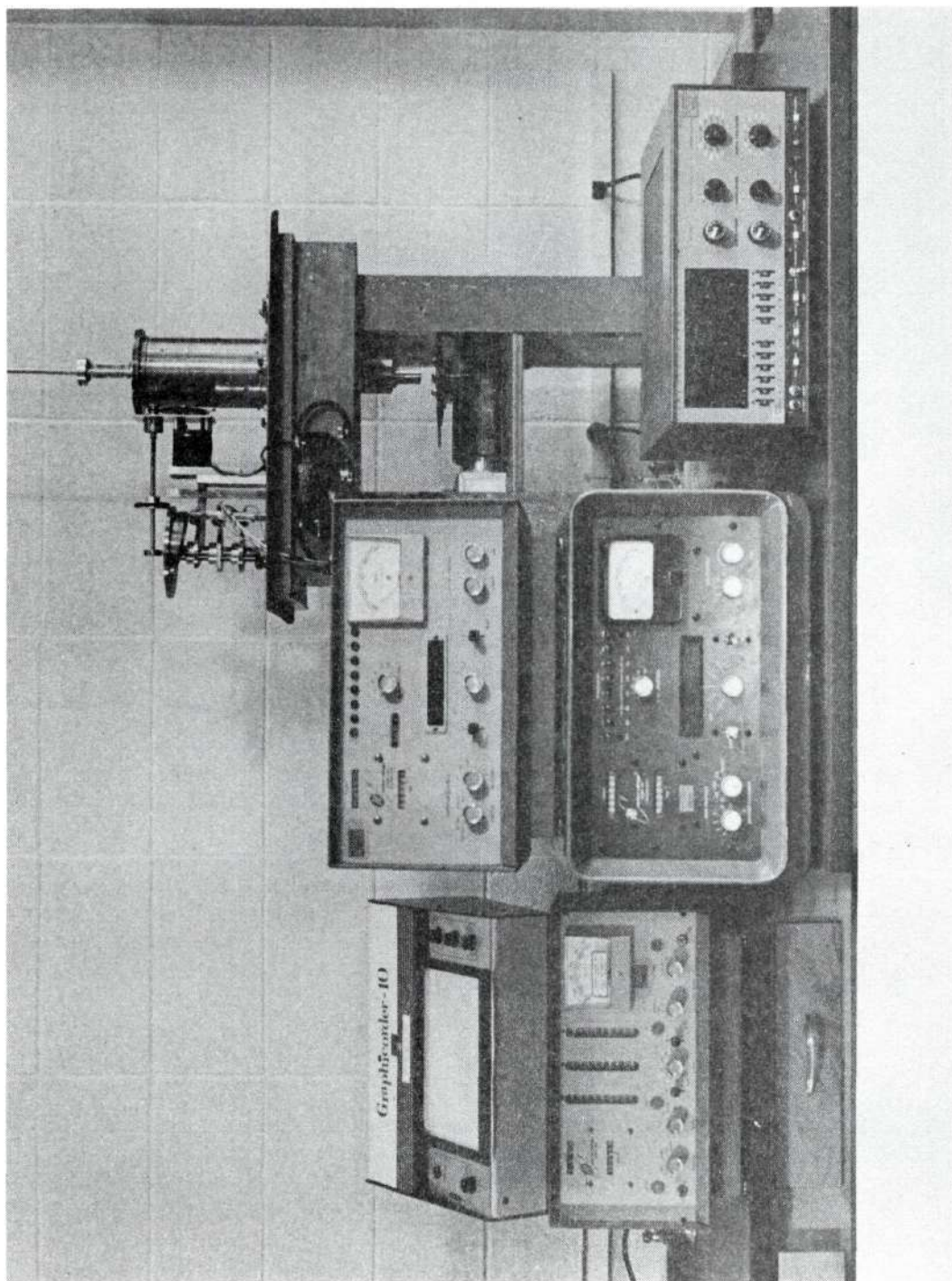


Figure 6. Mössbauer Effect Spectrometer.

Procedure

All clay samples were powdered to at least less than $44\ \mu$. Sample holders were brass washers about 1 inch in diameter with an 0.5 inch center hole and ranging in thickness from 0.020 inches to 0.040 inches. A piece of 0.00025 inch mylar is glued to one side of the washer, the clay sample packed into the hole, and a second piece of mylar is glued to the washer to cover the clay and hold it in place. Thicknesses should be determined by the amount of iron in a sample. Those samples with a low iron content can be thicker than samples of a high iron content. Each sample must be run for a sufficient period of time (determined by the number of counts to be collected) to insure that statistical errors are low. For this work, from 50,000 to 100,000 counts were collected for a given velocity. The velocity is then changed to a new value and the procedure is repeated until the entire spectrum is measured.

CHAPTER III

DISCUSSION OF RESULTS

In the literature review the characteristic isomer shift and quadrupole splitting of Fe^{57} in a compound was discussed. The isomer shifts, expressed in mm/second, mentioned hereafter will be referred to the center of the six-line spectrum for metallic iron. The center of the absorption spectrum for metallic iron in this work occurred at - 0.25 mm/second. Values reported for the center of an absorption spectrum (isomer shift location) will have had 0.25 mm/second added to them. The quadrupole splittings reported for this work will be the absolute value for half the peak separation of a doublet. Table 1 contains the parameters determined in this work. Chemical formulas for the clay minerals were supplied by Charles E. Weaver, Professor of Geology, Georgia Institute of Technology.

The data indicate that it is possible to differentiate the trioctahedral clays from the dioctahedral clays. Values for isomer shifts and quadrupole splittings of the iron in the octahedral layers tend to be larger for the trioctahedral clays. Pollak, et al., (1962) have discussed the differences in octahedral sites due to the location of the hydroxyl ions in biotite. The dioctahedral clays tend to have the like octahedral sites filled. The trioctahedral clays have both like and unlike sites filled which affords two slightly different environments.

Table 1. Mössbauer Parameters Determined in This Work for
Clays and Associated Minerals

mm/second \pm 0.05

<u>Clay</u>	<u>Oxidation State</u>	<u>Isomer Shift</u>	<u>Quadrupole Splittings</u>
		mm/sec. \pm 0.05	mm/sec. \pm 0.05
<u>2:1 Dioctahedral</u>			
Nontronite	Fe ⁺³	$\sim + 0.43$	~ 0.24
Illite	Fe ⁺²	$\sim + 1.075$	~ 1.075
	Fe ⁺³	$\sim + 0.325$	~ 0.325
Glaucconite	Fe ⁺²	$\sim + 1.15$	~ 1.10
	Fe ⁺³	$\sim + 0.35$	~ 0.30
Montmorillonite < 0.2 μ	Fe ⁺³	Broad peak with apex at 0.2	
<u>2:1 Chain</u>			
Xylotile	Fe ⁺²	$\sim + 1.2$	~ 1.0
	Fe ⁺³	---	---
Attapulgit	Fe ⁺²	$\sim + 0.975$	~ 1.175
	Fe ⁺³	$\sim + 0.3$	~ 0.2
<u>1:1 Trioctahedral</u>			
Chamosite	Fe ⁺²	$\sim + 1.10$	~ 1.25
	Fe ⁺³	$\sim + 0.32$	~ 0.375
Cronstedtite	Fe ⁺²	$\sim + 1.10$	~ 1.05

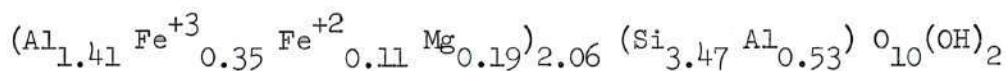
Table 1. (Continued)

<u>Clay</u>	<u>Oxidation State</u>	<u>Isomer Shift</u>	<u>Quadrupole Splittings</u>
		mm/sec. \pm 0.05	mm/sec. \pm 0.05
	Fe ⁺³	$\sim + 0.225$	~ 0.17
<u>2:1 Trioctahedral</u>			
Biotite Single Crystal	Fe ⁺²	+ 1.15	1.20
	Fe ⁺³		$\sim 0.2 - 0.6$
Biotite powder	Fe ⁺²	+ 1.15	1.20
Ferrionite (synthetic Biotite)	Fe ⁺²	+ 1.10	1.20
	Fe ⁺³	+ 0.05 or more	0.4 or less
Griffithite	Fe ⁺²	+ 1.15	1.30
	Fe ⁺³	$\sim + 0.40$	~ 0.55
<u>1:1 Dioctahedral</u>			
Iron Kaolin	Fe ⁺³	+ 0.375	0.225
<u>Iron Minerals</u>			
Goethite	Fe ⁺³	+ 0.375	0.275
Siderite	Fe ⁺²	+ 1.25	0.90

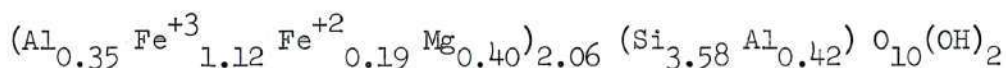
Clay Samples

2:1 Dioctahedral (Figure 7).

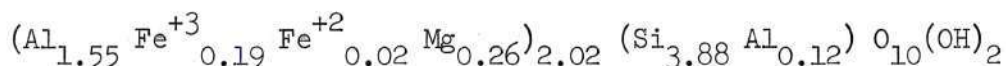
Illite Fe_2O_3 - 6.60% FeO - 1.87%



Glaucanite Fe_2O_3 - 20.0% FeO - 3.1%



Montmorillonite Fe_2O_3 - 3.67% FeO - 0.30%



Nontronite Fe_2O_3 - 31.24% FeO - 0.39%



The 2:1 dioctahedral clays provide some of the best spectra and information useful to determinations of other clay spectra. The nontronite spectrum shows a single peak in the zero velocity range with a width at half maximum of 0.95 mm/second. This can be decomposed into a quadrupole splitting doublet for Fe^{+3} with each peaking having approximately a half maximum width of 0.45 mm/second. The isomer shift of + 0.43 mm/second and quadrupole split value of approximately 0.24 mm/second from the decomposed peaks are within the accepted values for Fe^{+3} .

Except for the differences in the amount of absorption for each spectrum, glaucanite and illite are nearly identical and typical of most of the absorption spectra for the clay minerals with both Fe^{+3} and Fe^{+2} present. The glaucanite values of the isomer shift and quadrupole splitting of Fe^{+2} , + 1.15 mm/second and 1.10 mm/second, respectively, fall within

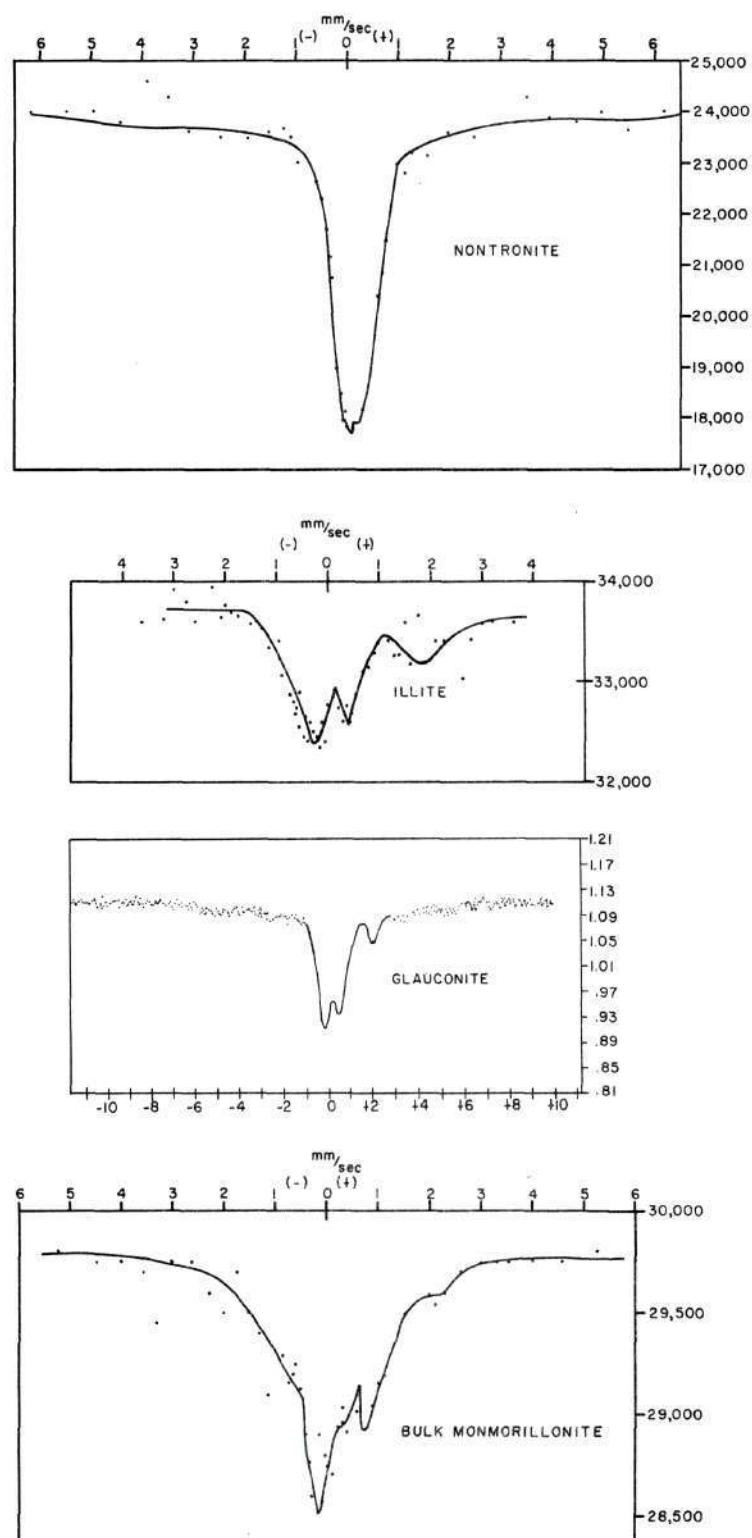


Figure 7. Mössbauer Spectra of 2:1 Dioctahedral Clays
Vertical Scale in Counts/Minute.

the reported values for the Fe^{+2} ion. Values for Fe^{+3} , + 0.35 mm/second isomer shift and 0.30 mm/second quadrupole split are within the defined range. Obtaining these values involved subtracting the absorption area due to Fe^{+2} located at 2.0 mm/second from the absorption area located at - 0.2 mm/second. The left peak of the Fe^{+2} doublet is in the same location (creating a stacking arrangement) as an Fe^{+3} split peak; in this instance at - 0.2 mm/second when the effect of the Fe^{+2} is subtracted from the - 0.2 mm/second absorption peak, the remaining area is equal to the peak at + 0.40 mm/second. These two peaks are attributed to the Fe^{+3} splitting.

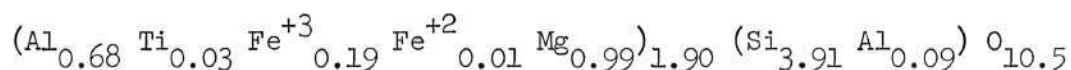
The same procedure applied to the spectrum for illite will yield a similar conclusion.

The spectrum for montmorillonite shows a broad peak with an apex at - 0.2 mm/second. It is quite obvious from examination of the spectrum that something more complex than well-defined shifts and splittings is occurring. Montmorillonite is the finest grained and most poorly crystallized of the samples, and a broadening effect should be expected. There are also indications of a complicating factor due to free iron oxides and hydroxides; however, a more thorough discussion of this will be taken up later.

A fine particle size fraction ($< 0.2 \mu$) was separated from the bulk clay and a spectrum determined. The percentage of absorption was small and only an indication of the Fe^{+3} doublet was observed.

2:1 Chain (Figure 8).

Attapulгите Fe_2O_3 - 3.36% FeO - 0.23%



Xylotile Fe_2O_3 - 16.7% FeO - 1.5%



The xylotile absorption spectrum presented a second case of interference due to an impurity; in this case it was siderite (FeCO_3). The x-ray pattern of the xylotile sample indicated the presence of siderite; however, attempts to remove it from the clay by heating the mixture in dilute HCl destroyed the clay as well as the siderite. This prompted the inclusion of another mineral to our list of clays being studied and the absorption spectrum for pure siderite was obtained. Values for the isomer shift and quadrupole splitting were + 1.25 mm/second and 0.90 mm/second respectively. The quadrupole split absorption peaks of the siderite (one at + 0.1 mm/second and one at + 1.9 mm/second), when removed from the xylotile spectrum, indicates the spectrum should resemble the previously discussed spectra which contain both Fe^{+2} and Fe^{+3} . Chemical analysis of the sample indicates the Fe^{+2} is a small percentage (1.5) and that for Fe^{+3} , 16.7 percent is present. Values of approximately 1.2 mm/second and 1.0 mm/second respectively for isomer shift and quadrupole splitting for Fe^{+2} can be determined from the spectrum. Siderite, however, does not allow resolution of the Fe^{+3} quadrupole splitting and the Fe^{+2} absorption appears high based on the chemical analysis. Either the chemical analysis is incorrect or the quadrupole splitting can be attributed to Fe^{+3} which would be larger than any mineral reported in the literature.

The spectrum for attapulgite required careful interpretation since

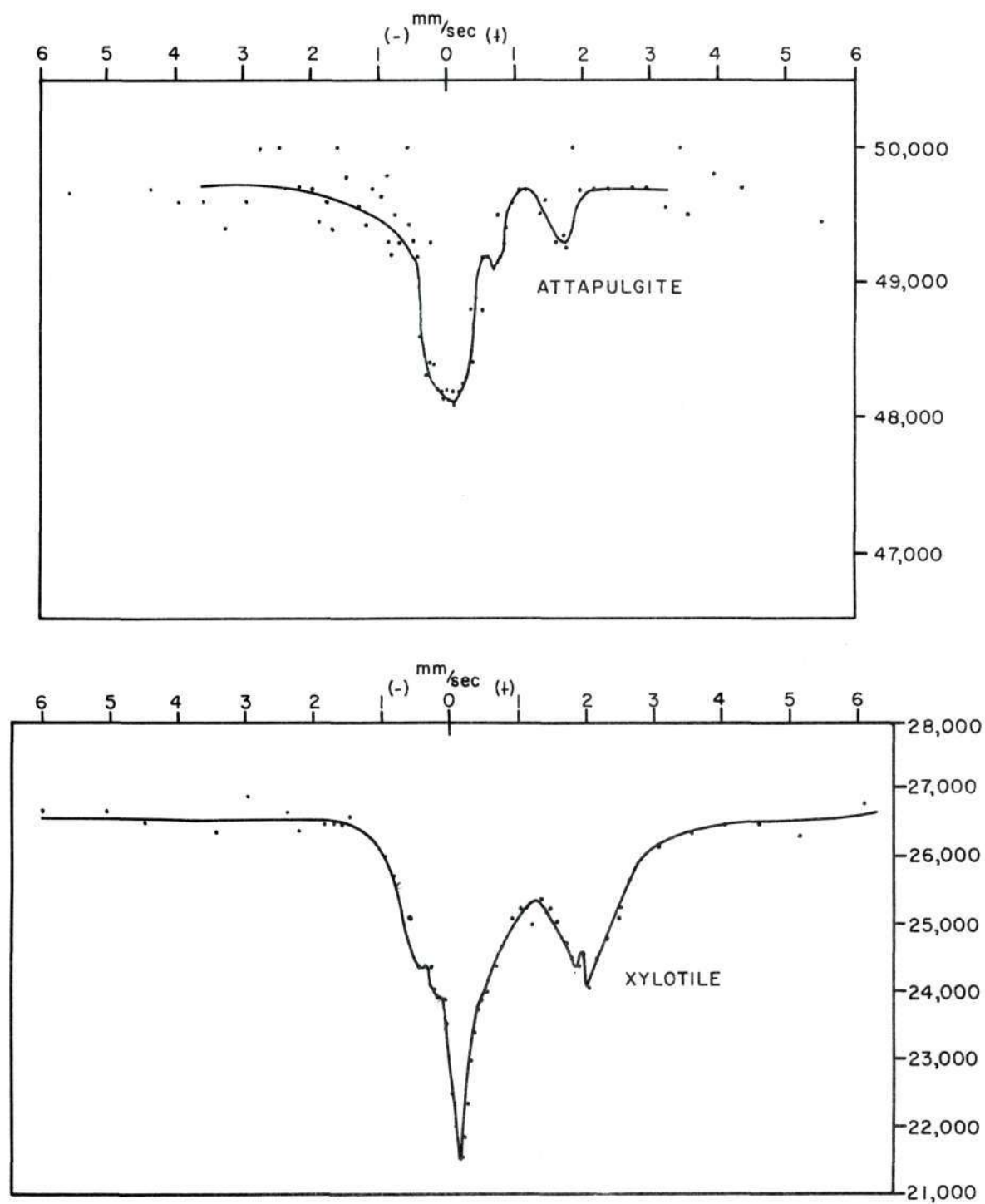


Figure 8. Mössbauer Spectra of Chain Structure Clays
Vertical Scale in Counts/Minute.

the sample had a small percentage of iron and background was higher than usual. The fact that both attapulgite and xylotile are 2:1 chain structures was very useful because of certain characteristics observed from the xylotile pattern. This made it possible to look for similar situations in the attapulgite. Fe^{+2} quadrupole splitting is present, as indicated by the absorption peak located at + 1.90 mm/second. The main peak near zero velocity is presumably due to an unresolved Fe^{+3} quadrupole doublet.

1:1 Trioctahedral (Figure 9).

Chamosite Fe_2O_3 - 0.23% FeO - 39.45%

$(\text{Al}_{0.85} \text{Fe}^{+3}_{0.01} \text{Fe}^{+2}_{1.84} \text{Mg}_{0.22})_2.92 (\text{Si}_{1.38} \text{Al}_{0.67}) \text{O}_5(\text{OH})_4$

Cronstedtite Fe_2O_3 29.72% FeO - 41.86%

$(\text{Fe}^{+3}_{0.71} \text{Fe}^{+2}_{2.38})_3.09 (\text{Si}_{1.12} \text{Al}_{0.07} \text{Fe}^{+3}_{0.41}) \text{O}_5(\text{OH})_4$

The chamosite spectrum indicates the presence of both Fe^{+2} and Fe^{+3} . Subtraction of the Fe^{+2} contribution leaves a Fe^{+3} doublet which is larger (amount of absorption) than expected. The chemical analysis indicates only 0.23 percent Fe^{+3} present. We may be experiencing absorption due to free iron oxides and hydroxides as mentioned earlier, or more Fe^{+3} may be in the lattice than indicated by the chemical formula. It is possible that the contamination is from mixed iron oxides, because the sample came from an oolitic iron stone.

The cronstedtite absorption spectrum has deep absorption peaks but they are rounded and smoothed by considerable overlapping. The chemical analysis shows a total of approximately 70 percent iron in the sample. Unfortunately, even making the sample very thin (although not as thin as possible) did not provide good resolution. It is possible, however, to

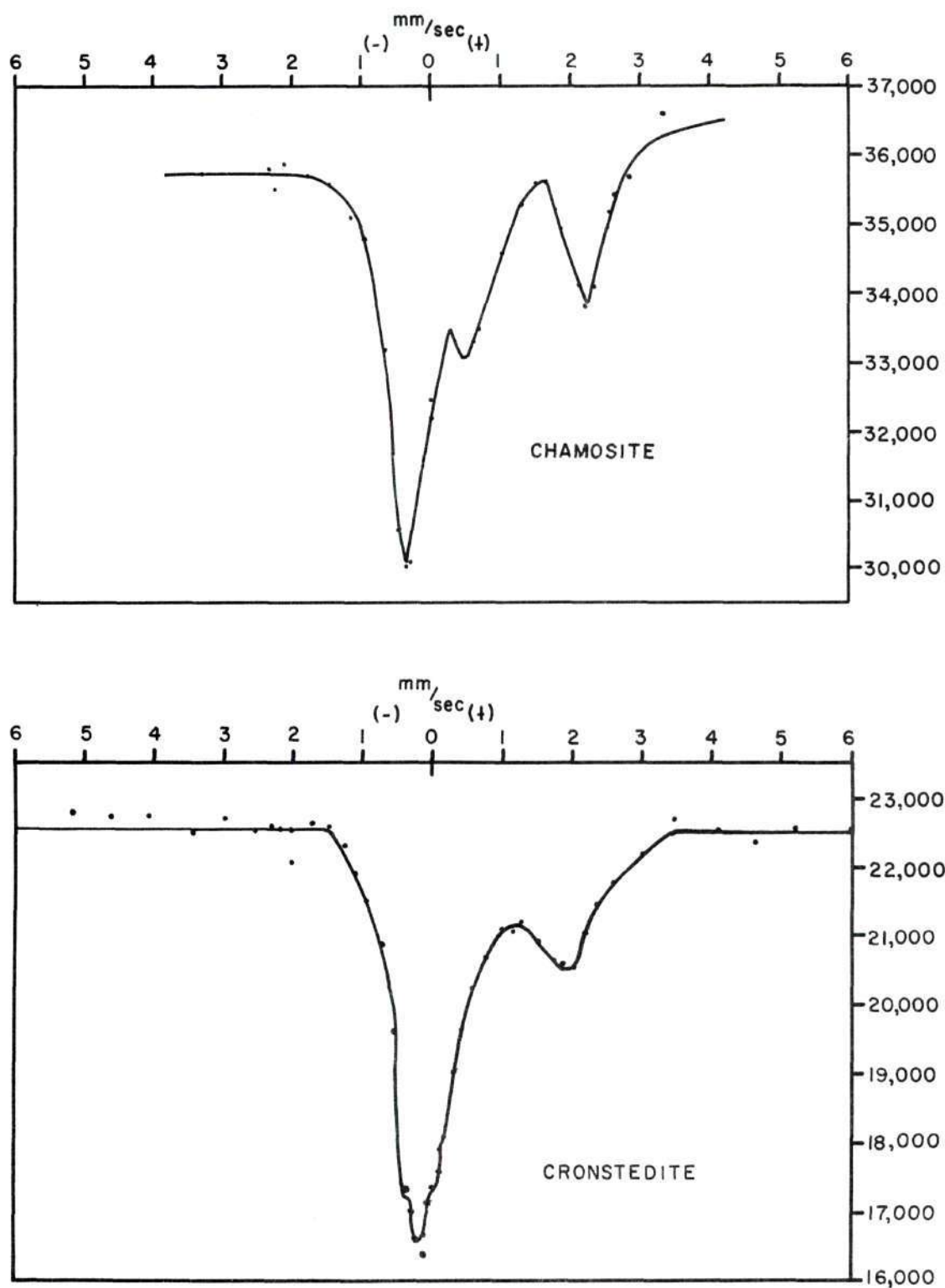


Figure 9. Mössbauer Spectra of 1:1 Trioctahedral Clays
Vertical Scale in Counts/Minute.

assume that the main absorption peak at - 0.20 mm/second may be a combination of the Fe^{+3} quadrupole split and very possibly two Fe^{+2} peaks stacked nearly on top of each other. This second consideration is made by resolving the broad absorption area at 2 mm/second into two Fe^{+2} quadrupole components. Another possible explanation may be the occurrence of Fe^{+3} in both tetrahedral and octahedral coordination with separate but unresolvable spectra. Admixed limonite was removed from the sample before preparation; however, microscopic examination of the sample indicated 0.1 - 0.3 percent siderite present. No attempt was made to remove it since very little success was had with previous removal attempts and the amount of sample was very small. In view of the fact that it was a small percentage of iron, compared to the total iron content of the sample, its effect was considered too negligible.

2:1 Trioctahedral Minerals (Figures 10 and 11).

Griffithite Fe_2O_3 7.32% FeO - 7.83%

$(\text{Al}_{0.04} \text{Fe}^{+3}_{0.52} \text{Fe}^{+2}_{0.44} \text{Mg}_{1.88})_{2.88} (\text{Si}_{3.19} \text{Al}_{0.81}) \text{O}_{10}(\text{OH})_2$

Ferrianite (Synthetic Biotite)

$\text{K Fe}^{+2}_3 \text{Fe}^{+3} \text{Si}_3 \text{O}_{10}(\text{OH})_2$

Biotite

$\text{K Fe}^{+2}_3 \text{Al Si}_3 \text{O}_{10}(\text{OH})_2$

Three variations of a biotite sample were run: a single crystal, a powdered sample of the single crystal material, and a synthetic biotite (ferriannite, $\text{K Fe}^{+2}_3 \text{Fe}^{+3} \text{Si}_3 \text{O}_{10}(\text{OH})_2$) supplied by David R. Wones, United States Department of the Interior, Geological Survey, Washington, D. C.

The two main peaks of the biotite spectrum are due to the quadrupole splitting of the octahedral Fe^{+2} . The line width at half height of the 2.10 mm/second peak is larger than that of the - 0.30 peak. Pollak, et al., (1962) considered this to be due to the two slightly different octahedral sites, both of which produced quadrupole splitting. At the negative velocity position these peaks are superimposed at the positive position. They are slightly offset, producing peak broadening.

The single crystal spectrum for biotite suggested the presence of the Fe^{+3} ion with the appearance of a small absorption peak at + 0.40 mm/second. When the same material was powdered, the distinct absorption peak for quadrupole split Fe^{+3} was replaced by a shoulder effect located at approximately the same position. The absorption peak for Fe^{+3} in the single crystal sample can be attributed to symmetry of the oriented sample. Broadening of the quadrupole split absorption peak for Fe^{+2} located at + 2.10 mm/second was noted. This may be due to the creation of a significant number of different octahedral sites at the edge of the powdered flakes.

The synthetic biotite (ferrianite) gives the first indications of a distinct spectrum for tetrahedrally coordinated Fe^{+3} ions. All Fe^{+3} is concluded to be in tetrahedral positions with only a slight possibility of any being present in octahedral sites. An absorption peak at + 0.20 mm/second is therefore attributed to tetrahedral Fe^{+3} and a shoulder effect at 0.50 - 0.60 mm/second may be from octahedral Fe^{+3} . The shoulder effect and distinct absorption peak at 0.50 - 0.60 mm/second in the powder biotite and single crystal biotite respectively, reinforce this conclusion.

Tetrahedral iron may be present in nontronite and cronstedtite;

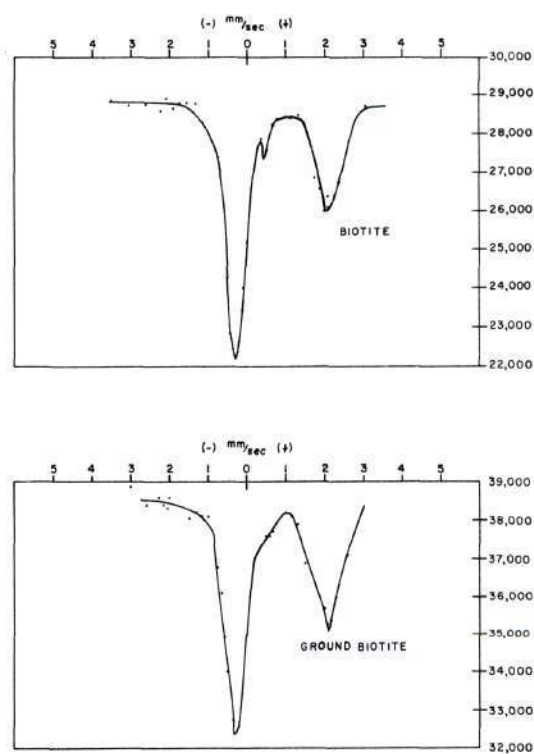


Figure 10. Mössbauer Spectra of Biotite
Vertical Scale in Counts/Minute.

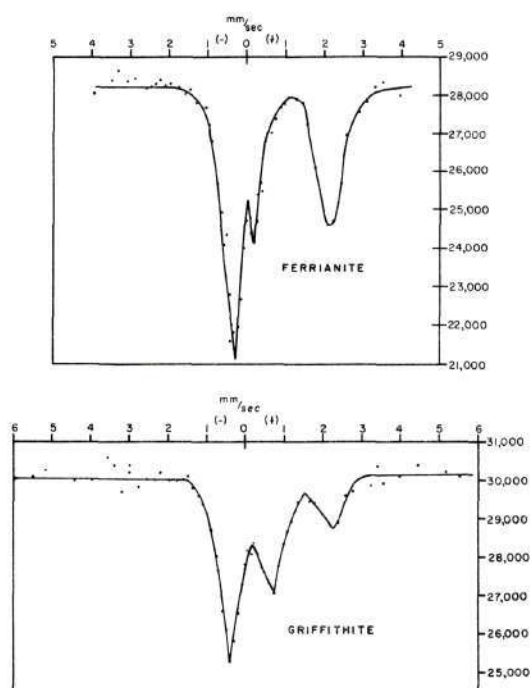


Figure 11. Mössbauer Spectra of Ferrianite and Griffithite
Vertical Scale in Counts/Minute.

however, there is so much peak overlap that a definite conclusion cannot be made on the basis of the present data.

Griffithite was the lone clay member of the 2:1 trioctahedrals and produced a similar though more widely spaced spectrum than other clays. The presence of Fe^{+2} and Fe^{+3} was easily noted, with the quadrupole splitting of Fe^{+3} giving a value of 0.55 mm/second which was the largest noted in this work. Isomer shifts and quadrupole splittings for Fe^{+2} were within the acceptable ranges. The spectrum was similar to biotite showing the effects of greater Fe^{+3} present; both Fe^{+2} and Fe^{+3} splittings were larger than the biotite as might be expected.

Iron Minerals (Figure 12).

Iron Kaolin Fe_2O_3 8.25% FeO - N.D.

$(\text{Al}_{1.63} \text{Fe}^{+3}_{0.29} \text{Mg}_{0.08})_2 \text{Si}_{2.00} \text{O}_5 (\text{OH})_4$

Siderite - FeCO_3

Goethite - $\text{FeO}(\text{OH})$

In almost all cases, the formation of clay minerals is accompanied by the formation of amorphous or slightly crystalline contaminating substances. The most abundant interfering substance related to this work are the iron oxides and hydroxides, whether present at the formation site or acquired through transportation and sedimentation. As stated in the introductory remarks, clays may contain iron in the lattice or as a coating or an admixture. The recently completed works of Herzenberg and Toms (1966) and Nakamura, et al., (1964) have shown that fine particles and gels of iron oxides and hydroxides have absorption spectra in the region of - 1 mm/second to + 1 mm/second, some showing distinct absorption peaks and

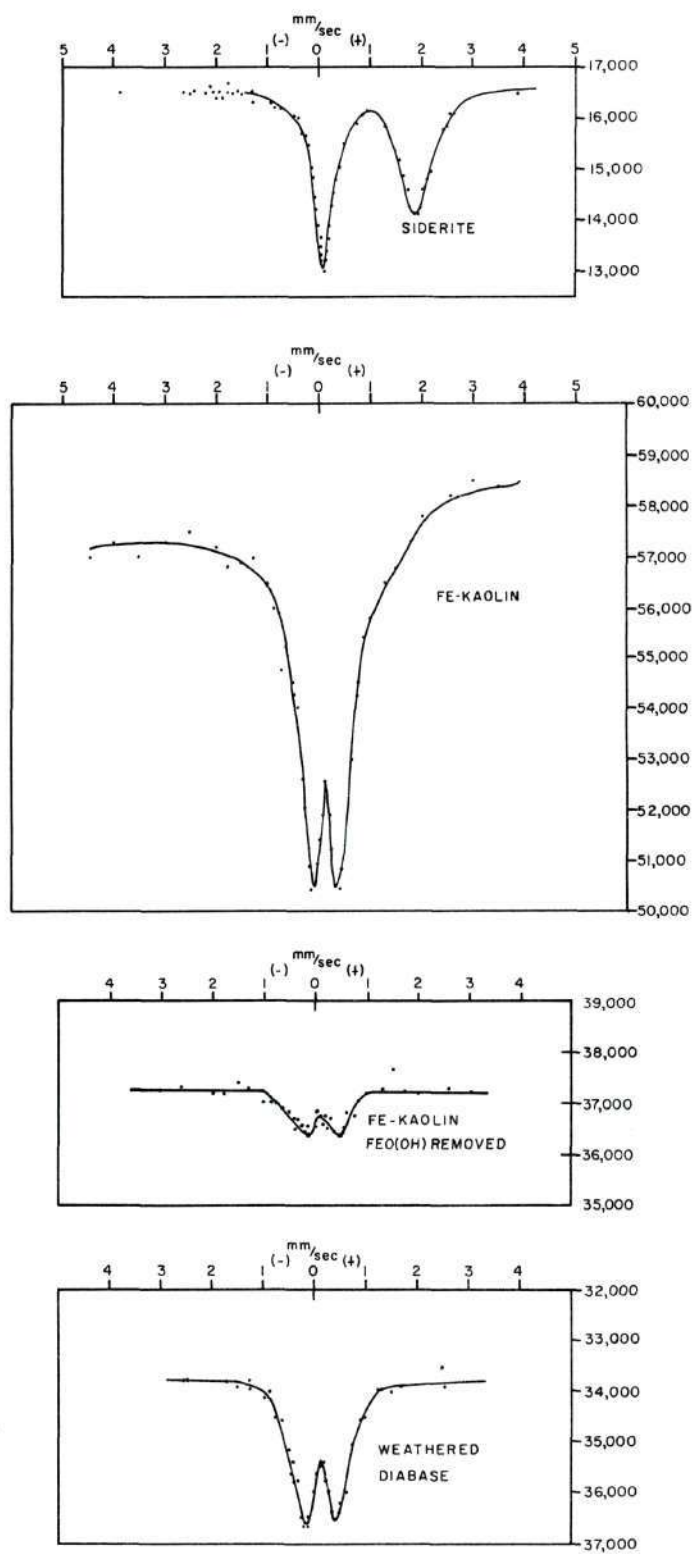


Figure 12. Mössbauer Spectra of Siderite, Fe-Kaolin and Goethite
Vertical Scale in Counts/Minute.

others just a large broad absorption dip.

A procedure to determine the extent of the effect in relation to our samples was taken up. A sample of weathered diabase (from a dike located about 10 miles east of Rock Hill, South Carolina) was run on the Mössbauer apparatus. An x-ray diffraction pattern of the sample gave a slight indication of a goethite peak (4.18A spacing) but most of the iron was amorphous to x-rays. The absorption spectrum is similar to one for βFeOOH (Herzenberg and Toms, 1966) and $\alpha\text{Fe}_2\text{O}_3$ (Nakamura, et al., 1964) and suggest the iron is better organized than indicated by the x-ray.

The second step of the procedure was to determine the absorption spectrum for an iron kaolin (Kunze and Bradley, 1963), $(\text{Al}_{1.63}\text{Fe}^{+3}_{0.29}\text{Mg}_{0.08})\text{Si}_{2.0}\text{O}_5(\text{OH})_4$. In order to account for the exchange capacity, they assumed that much of the iron was probably in the ferrous state.

The same sample was then treated to remove any free iron oxides (Jackson, 1956). After the removal of the iron oxides an x-ray diffraction pattern was run and another absorption spectrum.

From the original absorption spectrum it was evident that all the iron was in the Fe^{+3} valence state, and that the spectrum was identical to that of goethite. The removal of the free iron oxides also caused the destruction of most of the original absorption spectrum. The x-ray diffraction pattern which was as intense as the first pattern, indicated the presence of the (7.2A spacing) for kaolin, assuring that the clay had not been destroyed. It is possible that the method for removing the iron oxides may have preferentially attacked the iron kaolin and destroyed it while leaving an aluminum kaolin intact but without any iron in the lattice; however, it seems more likely that there is little, if any, iron

in the kaolin lattice and that it is present as very fine grained goethite.

Heating a portion of the untreated sample for two hours at 550°C removed the hydroxylions from the clay and may have initiated some crystallinity changes. The absorption spectrum showed a broadening of the absorption area. Indications are that this is caused by changes occurring in the iron oxyhydroxides and not the clay structure. The x-ray diffraction pattern for the sample indicated the goethite had been changed to hematite.

Determination of the siderite absorption spectrum to help resolve the xylotile absorption spectrum provided some interesting information concerning the equipment and sample preparation. Siderite (FeCO_3) provided a well spaced quadrupole split spectrum typical of the Fe^{+2} ion. Two absorption spectra were determined for the siderite based on two samples of different thicknesses. The first run was made with the thicker sample and the absorption peak at + 1.90 mm/second was not as deep and considerably broader than the quadrupole component at + 0.10 mm/second. Examination of the area under each absorption peak showed them to be equal. Explanations for peak broadening of the quadrupole component at 1.90 mm/second were essentially two; sample thickness and gamma-ray source location (distance from sample). A second sample was prepared of approximately one-tenth the thickness of the original sample. The gamma-ray source was moved twice the distance away from the sample as it had been in the original run. The completed spectrum was typical of pure quadrupole splitting with both peaks identical in shape and size (Figure 2). A schematic diagram of the gamma-ray source location showed that line broadening of the magnitude observed in the first siderite spectrum could not be attributable to source location (Figure 13). The source location does, however,

have a line broadening effect, though nearly negligible, and for future work a fixed position is advisable. It is concluded that the major contribution to line broadening was due to sample thickness. The problem of line broadening is a common one to all Mössbauer work (Preston, et al., 1962; Cordey-Hayes, et al., 1960).

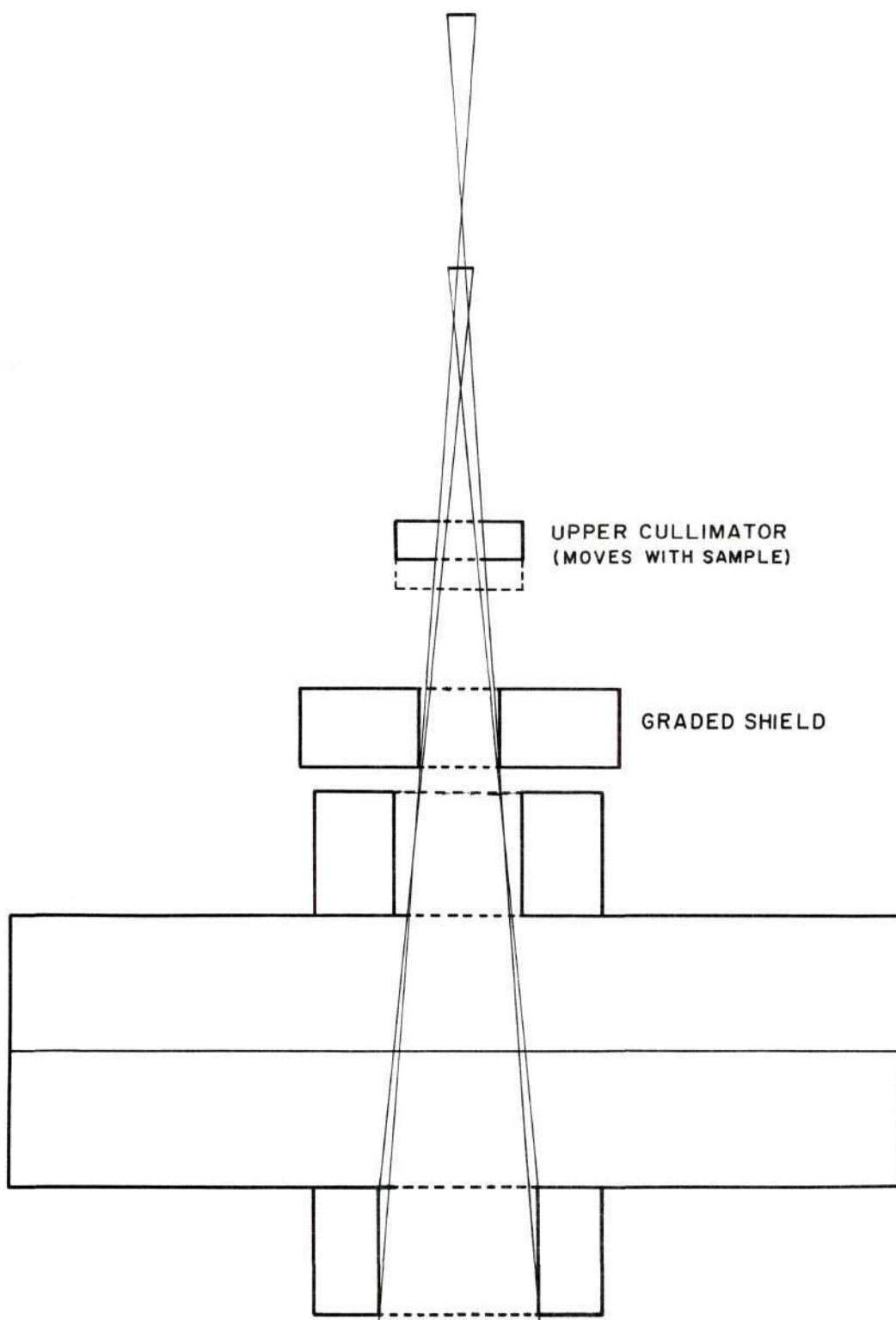


Figure 13. Schematic Diagram of the Gamma-ray Source Showing the Effect of Source Location on Line Broadening.

CHAPTER IV

CONCLUSIONS AND RECOMMENDATIONS

1. The use of Mössbauer spectroscopy to study iron in clay minerals is a practical method and should contribute considerable information on detailed structural variations in the clay minerals.
2. Samples with iron in only one oxidation state give distinct identifiable spectra.
3. Separation and identification of the oxidation states (Fe^{+2} and Fe^{+3}) of iron can be accomplished when both are present in a sample.
4. It should be possible to identify free iron oxides and hydroxides in a clay though they complicate spectrum interpretation.
5. It appears that tetrahedrally and octahedrally coordinated iron have slightly different spectra.
6. The trioctahedral clays can be distinguished from the dioctahedral clays.

The Following Improvements in Research Techniques are RecommendedA. Samples

1. Removal of free iron oxides and hydroxides, and other iron containing minerals from the clay minerals to insure pure samples.
2. A standardized sample preparation procedure based on either a standard thickness for all samples or a thickness determined by the iron content per unit area for each sample.

B. Equipment

1. Relinquishing the flexibility of a moveable gamma ray source in favor of a fixed position.

2. Constructing or procuring a constant velocity cam divided into three portions: positive velocity, negative velocity, and zero velocity to provide longer time intervals for collecting data. This would replace the quartered cam which has two zero velocity positions, one of which is unnecessary.

3. Making a momentary contact of the microswitches controlling the scalers.

C. Research

1. Additional work with the application of low temperature techniques to determine if spectra will be altered. This may provide a means for more precise separation and identification of mixed clays.

BIBLIOGRAPHY

1. Cordey-Hayes, M., Dyson, N. A., and Moon, P. B., "Width and Intensity of the Mössbauer Line in Iron-57," Proc. Phys. Soc., London, 75, 810, 1960.
2. DeBenedetti, S., Lang, G., and Ingalls, R., "Electric Quadrupole Splitting and the Nuclear Volume Effect in the Ions of Fe^{57} ," Phys. Rev. Letters, 6, 60, 1961.
3. DeCoster, M., Pollak, H., and Amelinckx, S., "A Study of Mössbauer Absorption in Iron Silicates," Phys. Stat. Sol. 3, 283, 1963.
4. Fluck, E., Kerler, W., and Neuwirth, W., "The Mössbauer Effect and its Significance in Chemistry," Angewandte Chemie 2, 277, 1963.
5. Frauenfelder, H., The Mössbauer Effect, W. A. Benjamin, Inc., New York, 1962.
6. Hanna, S. S., Heberle, J., Littlejohn, C., Perlow, G. J., Preston, R. S., and Vincent, D. H., "Polarized Spectra and Hyper-fine Structure in Fe^{57} ," Phys. Rev. Letters 4, 177, 1960.
7. Herzenberg, C. L., and Toms, D., "Mössbauer Absorption Measurements in Iron-Containing Minerals," Jour. of Geophys. Res. 71, 2661, 1966.
8. Jackson, M. L., "Soil Chemical Analysis - Advanced Course," published by the Author, Department of Soils, University of Wisconsin, Madison, Wisconsin, 1956.
9. Kistner, O. C., and Sunyar, A. W., "Evidence for Quadrupole Interaction of Fe^{57} and Influence of Chemical Binding on Nuclear Gamma Ray Energy," Phys. Rev. Letters 4, 412, 1960.
10. Mössbauer, R. L., "Dernresonanzfluoreszenz von Gammastrahlung in Ir^{191} ," Z. Phys., 151, 124, 1958.
11. Nakamura, T., Shinjo, T., Endoh, Y., Yamamoto, N., Shiga, M., and Nakamura, Y., " Fe^{57} Mössbauer Effect in Ultra Fine Particles of $\alpha\text{-Fe}_2\text{O}_3$," Phys. Letters 4, 178, 1965.
12. Preston, R. S., Hanna, S. S., and Heberle, J., "Mössbauer Effect in Metallic Iron," Phys. Rev., 128, 2207, 1962.
13. Pollak, H., DeCoster, M., and Amelinckx, S., "Mössbauer Effect in Biotite," Phys. Stat. Soc. 2, 1653, 1962.

14. Sprenkel-Segel, E. L., and Hanna, S. S., "Mössbauer Analysis of Stone Meteorites," Geochimica Cosmochimica Acta 28, 1913, 1964.
15. Walker, L. R., Wertheim, G. K., and Jaccarino, V., "Interpretation of the Fe^{57} Isomer Shift," Phys. Rev. Letters 6, 98, 1961.
16. Wertheim, G. K., "Resource Letter ME-1 on the Mössbauer Effect," Am. Jour. Phys. 31, 1, 1963.
17. Wertheim, G. K., Mössbauer Effect, Academic Press, New York, 1964.